

Electronic Supplementary Information

Potential SiX (X = N, P, As, Sb, Bi) homo-bilayers for visible-light photocatalysts application

Radha N Somaiya¹, Deobrat Singh^{2,*}, Yogesh Sonvane^{1,*}, Sanjeev K. Gupta^{3,*}, and Rajeev Ahuja^{2,4}

¹Advanced Materials Lab, Department of Physics, Sardar Vallabhbhai National Institute of Technology, Surat 395007, India

²Condensed Matter Theory Group, Materials Theory Division, Department of Physics and Astronomy, Uppsala University, Box 516, 75120 Uppsala, Sweden

³Computational Materials and Nanoscience Group, Department of Physics, St. Xavier's College, Ahmedabad 380009, India

⁴Applied Materials Physics, Department of Materials Science and Engineering, Royal Institute of Technology (KTH), S-100 44 Stockholm, Sweden

Tables Caption:

Table. S1 Calculated lattice parameters for the hexagonal SiX bilayers with different stacking configurations.

Table. S2 Calculated parameters for the hexagonal SiX homo-bilayers with different stacking configurations via GGA-PBE.

Table. S3 Calculated parameters for the hexagonal SiX homo-bilayers with different stacking configurations via DFT-D2.

Table. S4 Indicating the calculated carrier mobilities of group IV-V SiX monolayers at 300 K along the x- and y- direction with PBE functional.

Table. S5 Calculated values of the electronegativities, energy band gap, valence band and the conduction band potentials of SiX monolayer.

Table. S6 Indicates the adsorption energies (ΔE_{ad}) in eV of intermediates O*, OH*, and OOH* on SiP and SiAs homo-bilayer at different sites.

Figures Caption:

Fig. S1 Indicates the orthogonal supercell for stable SiX homo-bilayers to study the transport properties along x- and y-directions with the corresponding Brillouin zone for orthorhombic lattice.

Fig. S2 Phonon dispersion spectrum of group-IV and V homo-bilayers viz. (a) SiN, (b) SiP, (c) SiAs, (d) SiSb, and (e) SiBi for five different stackings plotted at high symmetric points in the Brillouin zone.

Fig. S3 Molecular dynamics simulations indicating evolution of total energy vs time and the snapshots of the top views of the structures initially at 0 K and optimized structure at 300 K for (a) SiN, (b) SiP, (c) SiAs, (d) SiSb, and (e) SiBi homo-bilayers respectively for five different stackings. Green and purple balls indicate Si and X (X=N, P, As, Sb, Bi) atoms respectively.

Fig. S4 Indicates the electronic band structures and the projected density of states of group IV-V homo-bilayers of (a) SiN, (b) SiP, (c) SiAs, (d) SiSb, and (e) SiBi calculated with both PBE functional (solid blue line) and HSE06 hybrid functional (solid red line) for the unstable stackings S-II and S-IV.

Fig. S5 Energy shift of VBM and CBM for homo-bilayers (a) SiN, (b) SiP, (c) SiAs, (d) SiSb, and (e) SiBi w.r.t. uniaxial compressive and tensile strains applied along the x- and y- directions for all the stable stacking configurations.

Fig. S6 Depicts the strain energy difference between the total energy of unstrained and strained homo-bilayers (a) SiN, (b) SiP, (c) SiAs, (d) SiSb, and (e) SiBi w.r.t. uniaxial compressive and tensile strains applied along the x- and y- directions for all the stable stacking configurations.

Fig. S7 The optimized structures of the adsorption of intermediates O*, OH*, and OOH* on the SiP homo-bilayer. The Si, X, O, and H atoms are represented by green, purple, red, and gray respectively.

Fig. S8 Indicates the calculated relaxation time for the studied homo-bilayers at different temperatures.

Fig. S9 Indicates the power factor plotted as a function of chemical potential at different temperatures.

Table S1

| System | Stacking | I | II | III | IV | V |
|---------------|-----------------|----------|-----------|------------|-----------|----------|
| SiN | No-vdW | 2.899 | 2.899 | 2.899 | 2.899 | 2.899 |
| | DFT-D2 | 2.895 | 2.894 | 2.894 | 2.894 | 2.895 |
| | DFT-D3 | 2.889 | 2.887 | 2.887 | 2.887 | 2.888 |
| SiP | No-vdW | 3.529 | 3.529 | 3.529 | 3.529 | 3.529 |
| | DFT-D2 | 3.520 | 3.520 | 3.522 | 3.520 | 3.521 |
| | DFT-D3 | 3.497 | 3.497 | 3.502 | 3.497 | 3.499 |
| SiAs | No-vdW | 3.696 | 3.696 | 3.697 | 3.696 | 3.696 |
| | DFT-D2 | 3.688 | 3.688 | 3.690 | 3.688 | 3.689 |
| | DFT-D3 | 3.664 | 3.661 | 3.668 | 3.661 | 3.664 |
| SiSb | No-vdW | 4.017 | 4.015 | 4.019 | 4.014 | 4.018 |
| | DFT-D2 | 4.014 | 4.026 | 4.019 | 4.018 | 4.016 |
| | DFT-D3 | 3.978 | 3.993 | 3.995 | 3.993 | 3.983 |
| SiBi | No-vdW | 4.171 | 4.169 | 4.179 | 4.168 | 4.176 |
| | DFT-D2 | 4.171 | 4.188 | 4.179 | 4.174 | 4.175 |
| | DFT-D3 | 4.132 | 4.148 | 4.146 | 4.129 | 4.139 |

Table S2

| System | Stacking | I | II | III | IV | V |
|---------------|-----------------|----------|-----------|------------|-----------|----------|
| SiN | a (Å) | 2.899 | 2.899 | 2.899 | 2.899 | 2.899 |
| | d (Å) | 3.917 | 4.489 | 4.273 | 4.547 | 4.241 |
| | ΔE (meV) | 0 | 1.65 | 1.22 | 1.71 | 0.46 |
| SiP | a (Å) | 3.529 | 3.529 | 3.529 | 3.529 | 3.529 |
| | d (Å) | 4.372 | 4.888 | 4.564 | 4.929 | 4.358 |
| | ΔE (meV) | 0 | 1.27 | 0.20 | 1.26 | 0.12 |
| SiAs | a (Å) | 3.696 | 3.696 | 3.697 | 3.696 | 3.696 |
| | d (Å) | 4.184 | 5.091 | 4.372 | 4.959 | 4.169 |
| | ΔE (meV) | 0.40 | 1.61 | 0 | 1.88 | 0.16 |
| SiSb | a (Å) | 4.017 | 4.015 | 4.019 | 4.014 | 4.018 |
| | d (Å) | 4.203 | 5.150 | 3.893 | 5.115 | 4.016 |
| | ΔE (meV) | 5.61 | 11.64 | 0 | 12.80 | 2.61 |
| SiBi | a (Å) | 4.171 | 4.169 | 4.179 | 4.168 | 4.176 |
| | d (Å) | 3.824 | 5.113 | 3.497 | 5.081 | 3.655 |
| | ΔE (meV) | 17.96 | 32.98 | 0 | 34.91 | 7.99 |

Table S3

| System | Stacking | I | II | III | IV | V |
|---------------|-----------------|----------|-----------|------------|-----------|----------|
| SiN | a (Å) | 2.895 | 2.894 | 2.894 | 2.894 | 2.895 |
| | d (Å) | 3.026 | 3.476 | 3.233 | 3.4994 | 3.112 |
| | ΔE (meV) | 0 | 44.05 | 24.13 | 45.33 | 11.27 |
| SiP | a (Å) | 3.520 | 3.520 | 3.522 | 3.520 | 3.521 |
| | d (Å) | 3.356 | 3.939 | 3.342 | 3.939 | 3.333 |
| | ΔE (meV) | 0.75 | 46.95 | 1.73 | 47.49 | 0 |
| SiAs | a (Å) | 3.688 | 3.688 | 3.690 | 3.688 | 3.689 |
| | d (Å) | 3.412 | 4.004 | 3.335 | 4.012 | 3.376 |
| | ΔE (meV) | 5.29 | 57.02 | 0 | 57.39 | 2.05 |
| SiSb | a (Å) | 4.014 | 4.026 | 4.019 | 4.018 | 4.016 |
| | d (Å) | 3.665 | 5.105 | 3.430 | 4.539 | 3.568 |
| | ΔE (meV) | 17.98 | 74.61 | 0 | 71.84 | 8.94 |
| SiBi | a (Å) | 4.171 | 4.188 | 4.179 | 4.174 | 4.175 |
| | d (Å) | 3.250 | 5.055 | 2.983 | 4.116 | 3.105 |
| | ΔE (meV) | 52.89 | 194.84 | 0 | 164.87 | 25.21 |

Table S4

| System | | m_x^* (m_0) | m_y^* (m_0) | C_x^{2D} (N/m) | C_y^{2D} (N/m) | E_d^x (eV) | E_d^y (eV) | μ_x ($10^4 cm^2 V^{-1} s^{-1}$) | μ_y ($10^4 cm^2 V^{-1} s^{-1}$) |
|---------------|---|----------------------|----------------------|---------------------|---------------------|-----------------|-----------------|--|--|
| SiN | e | 0.041 | 0.127 | 299.48 | 299.44 | 9.196 | 3.465 | 2.56 | 5.82 |
| | h | 0.006 | 8.133 | 299.48 | 299.44 | 3.286 | 4.073 | 44.72 | 0.02 |
| SiP | e | 0.064 | 1.374 | 135.11 | 135.07 | 5.370 | 1.434 | 0.53 | 0.35 |
| | h | 0.103 | 0.495 | 135.11 | 135.07 | 1.016 | 3.867 | 12.03 | 0.17 |
| SiAs | e | 0.116 | 0.640 | 111.68 | 111.53 | 1.759 | 2.112 | 2.44 | 0.31 |
| | h | 0.079 | 0.310 | 111.68 | 111.53 | 1.483 | 0.124 | 8.78 | 319.57 |
| SiSb | e | 0.091 | 2.139 | 84.04 | 83.98 | 5.479 | 3.015 | 0.15 | 0.02 |
| | h | 0.114 | 0.194 | 84.04 | 83.98 | 2.128 | 2.723 | 2.34 | 0.84 |
| SiBi | e | 0.110 | 0.676 | 68.70 | 69.40 | 0.583 | 3.465 | 14.40 | 0.07 |
| | h | 0.093 | 0.269 | 68.70 | 69.40 | 0.159 | 4.073 | 394.85 | 0.21 |

Table S5

| <i>System</i> | χ | E_g | E_{CB} | E_{VB} |
|---------------|--------|-------|----------|----------|
| <i>SiN</i> | 5.902 | 2.711 | 0.047 | 2.758 |
| <i>SiP</i> | 5.173 | 2.186 | -0.420 | 1.766 |
| <i>SiAs</i> | 5.033 | 2.261 | -0.598 | 1.664 |
| <i>SiSb</i> | 4.813 | 1.756 | -0.565 | 1.191 |
| <i>SiBi</i> | 4.430 | 1.151 | -0.646 | 0.506 |

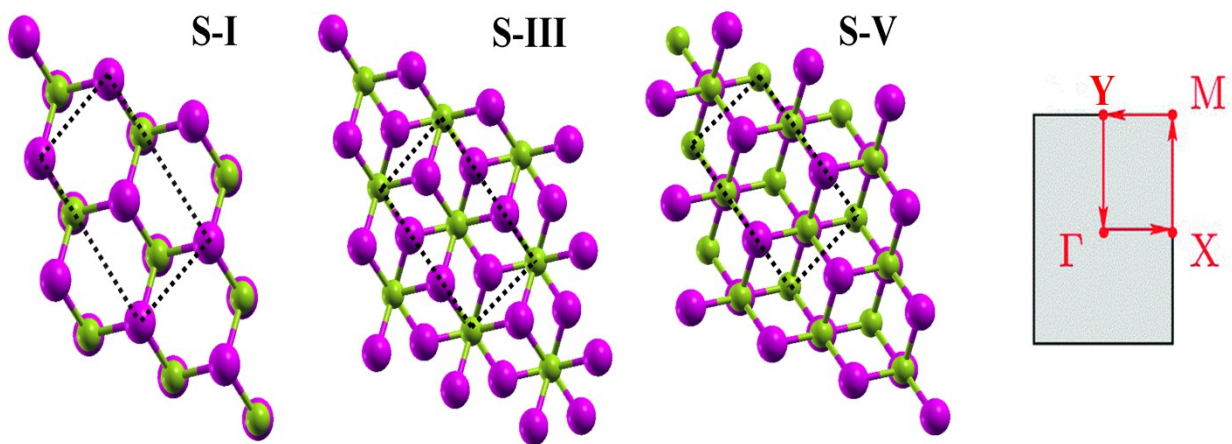


Fig. S1

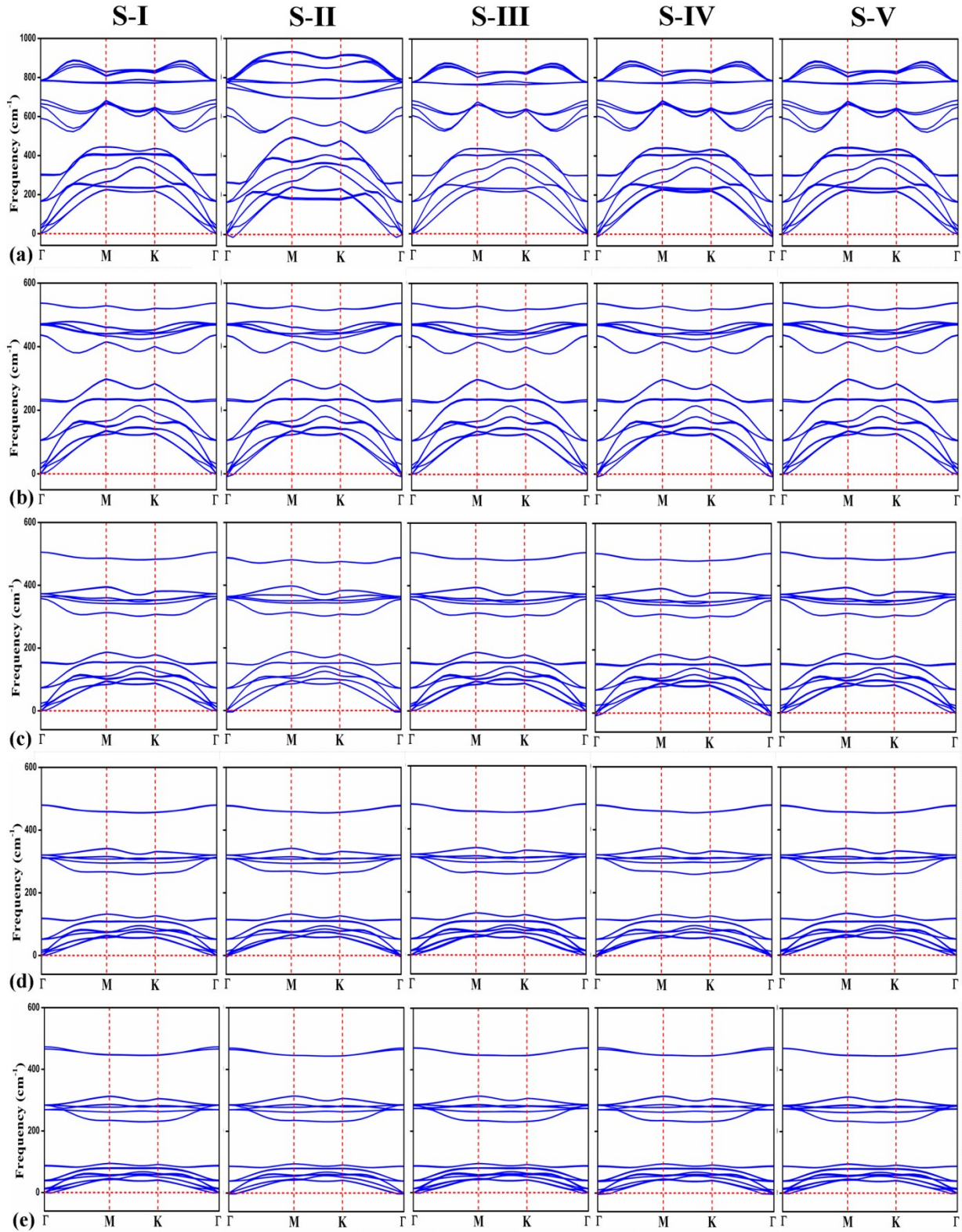
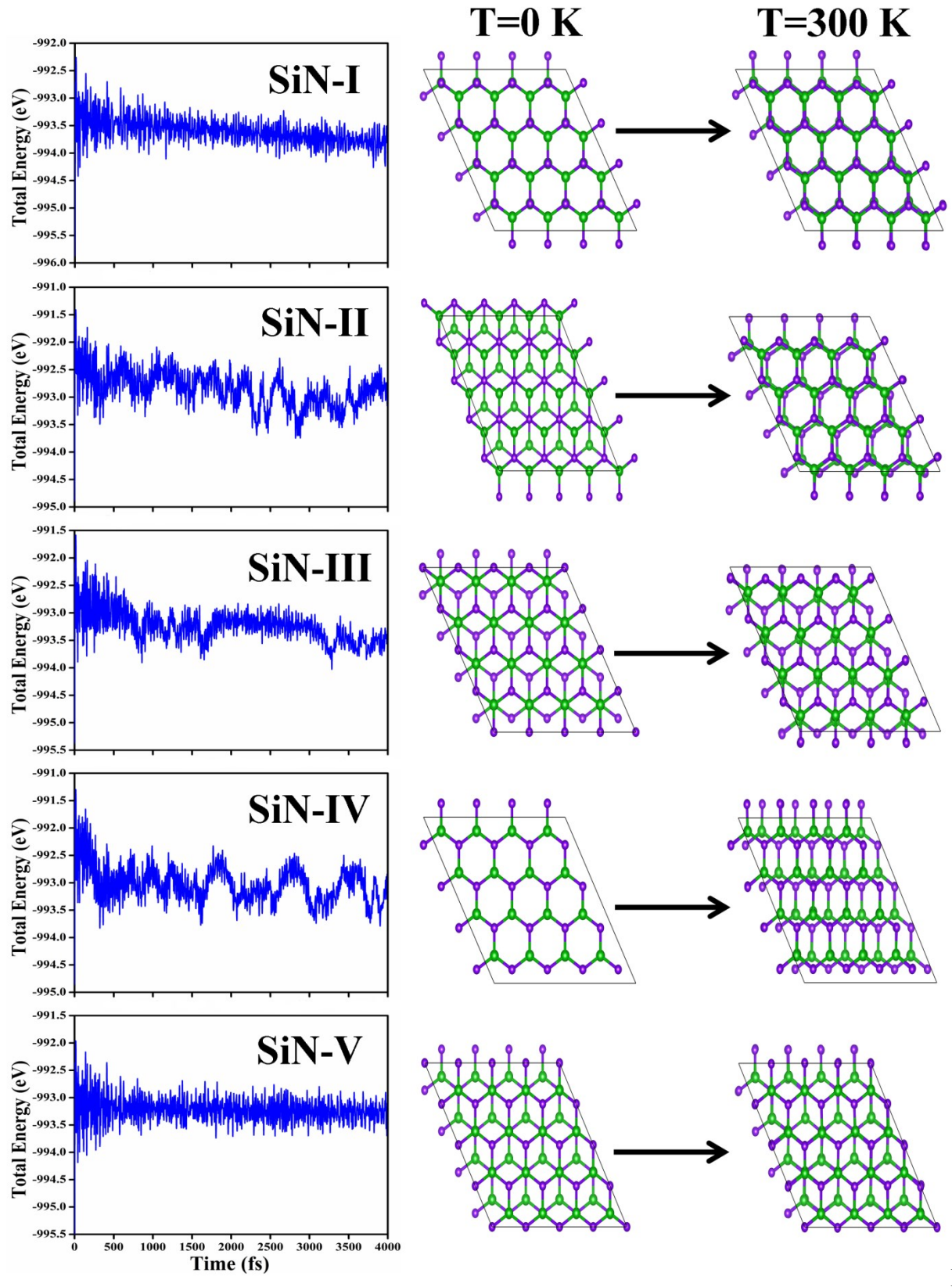
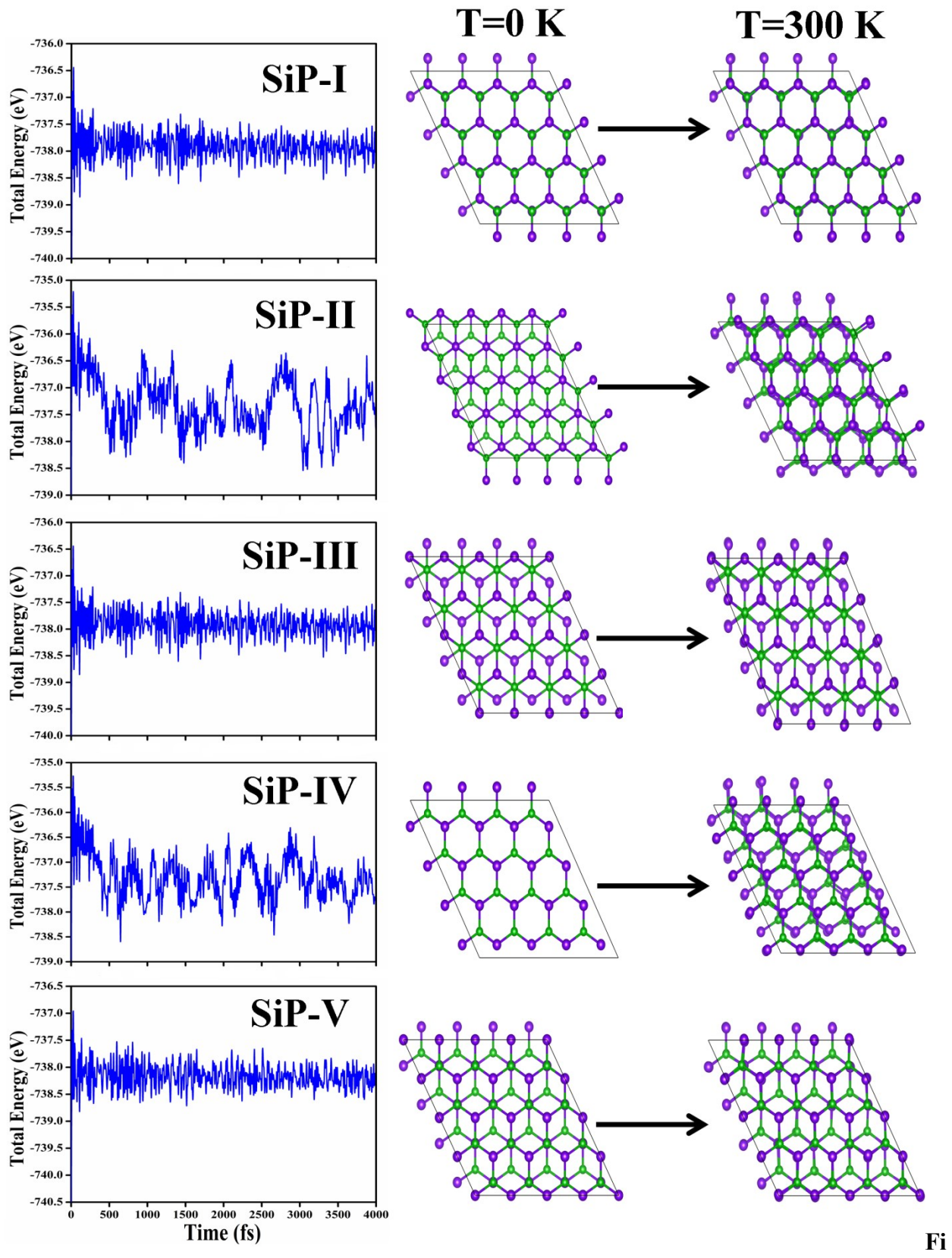


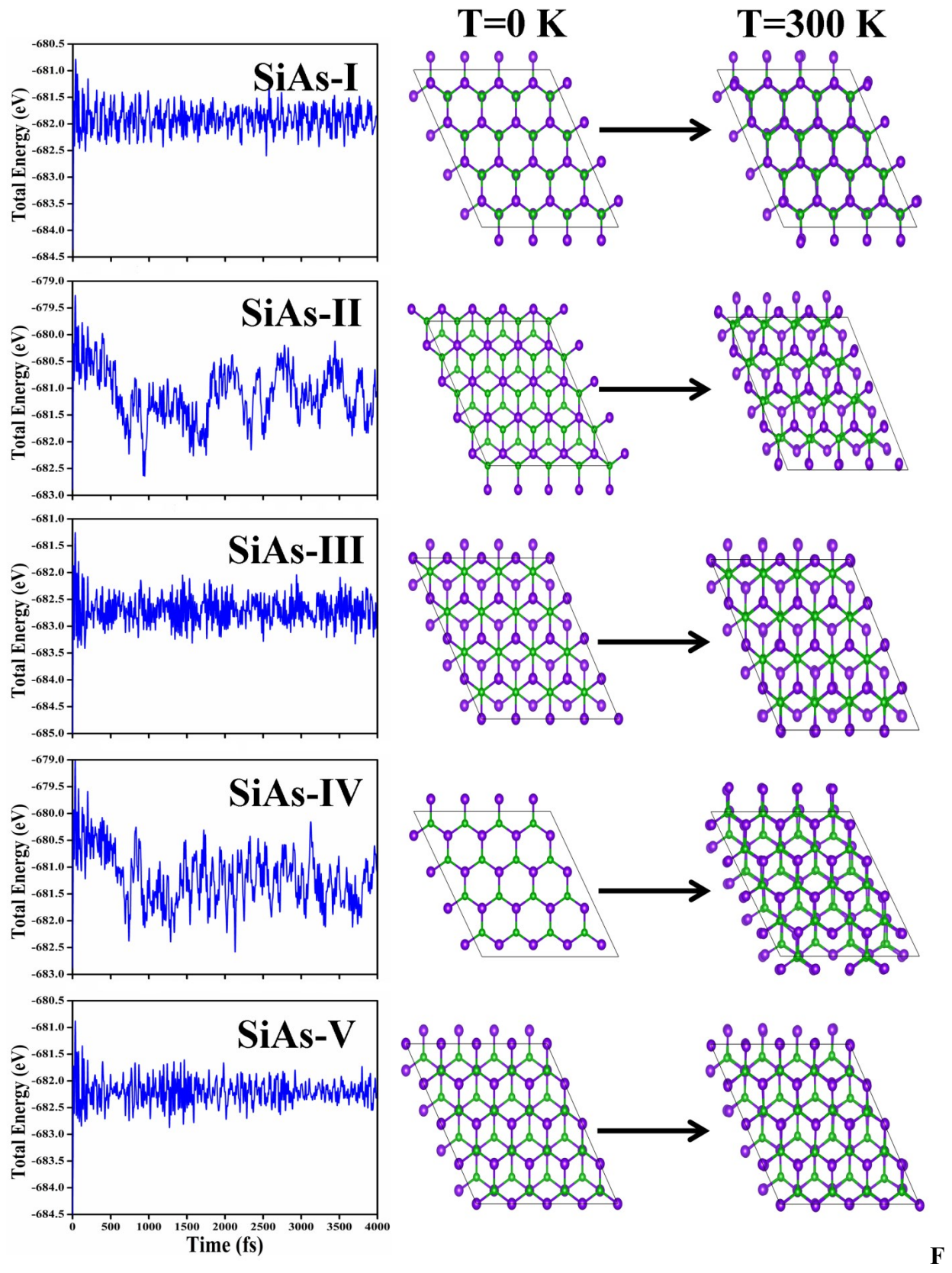
Fig. S2



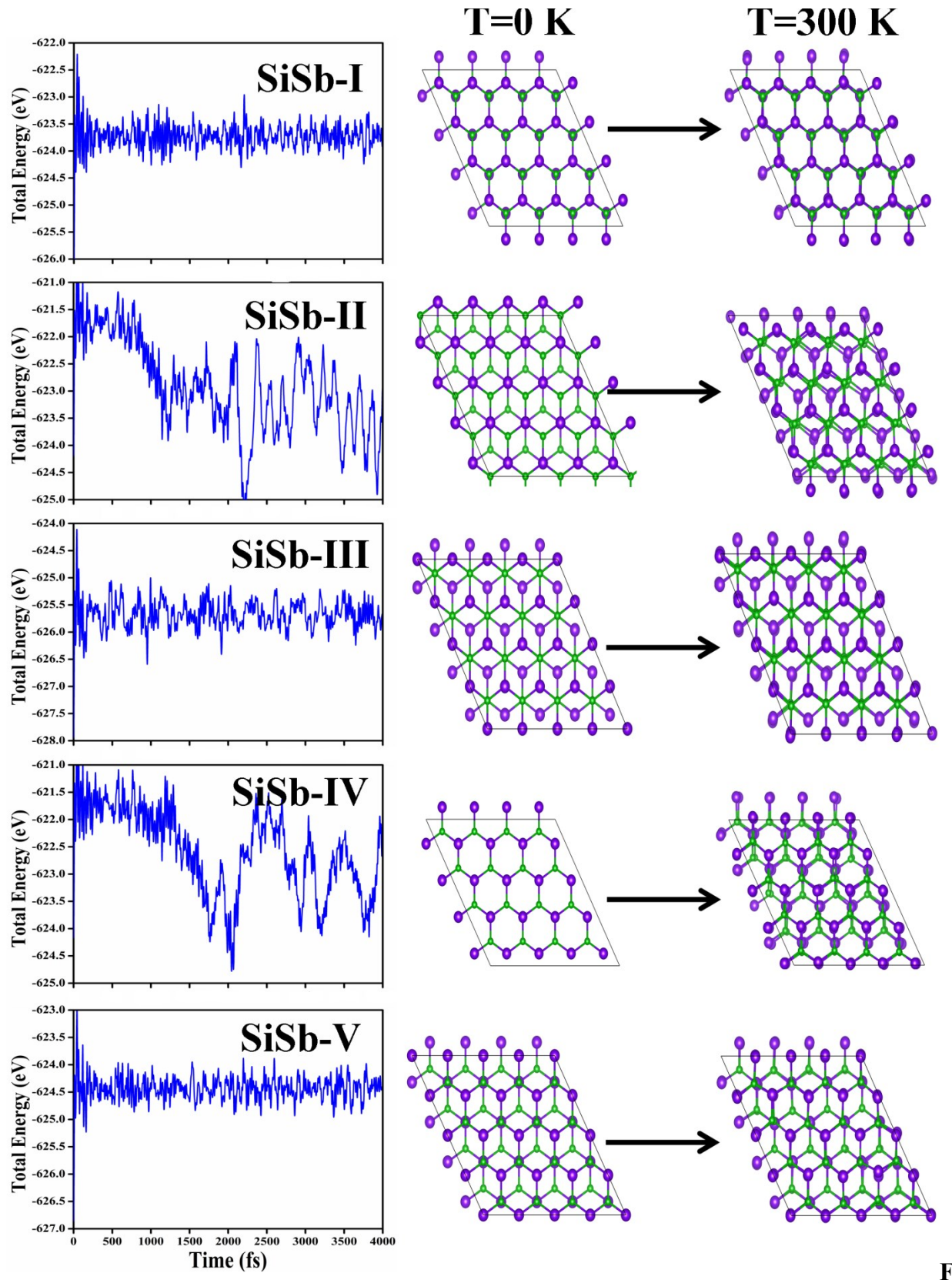
ig. S3(a)



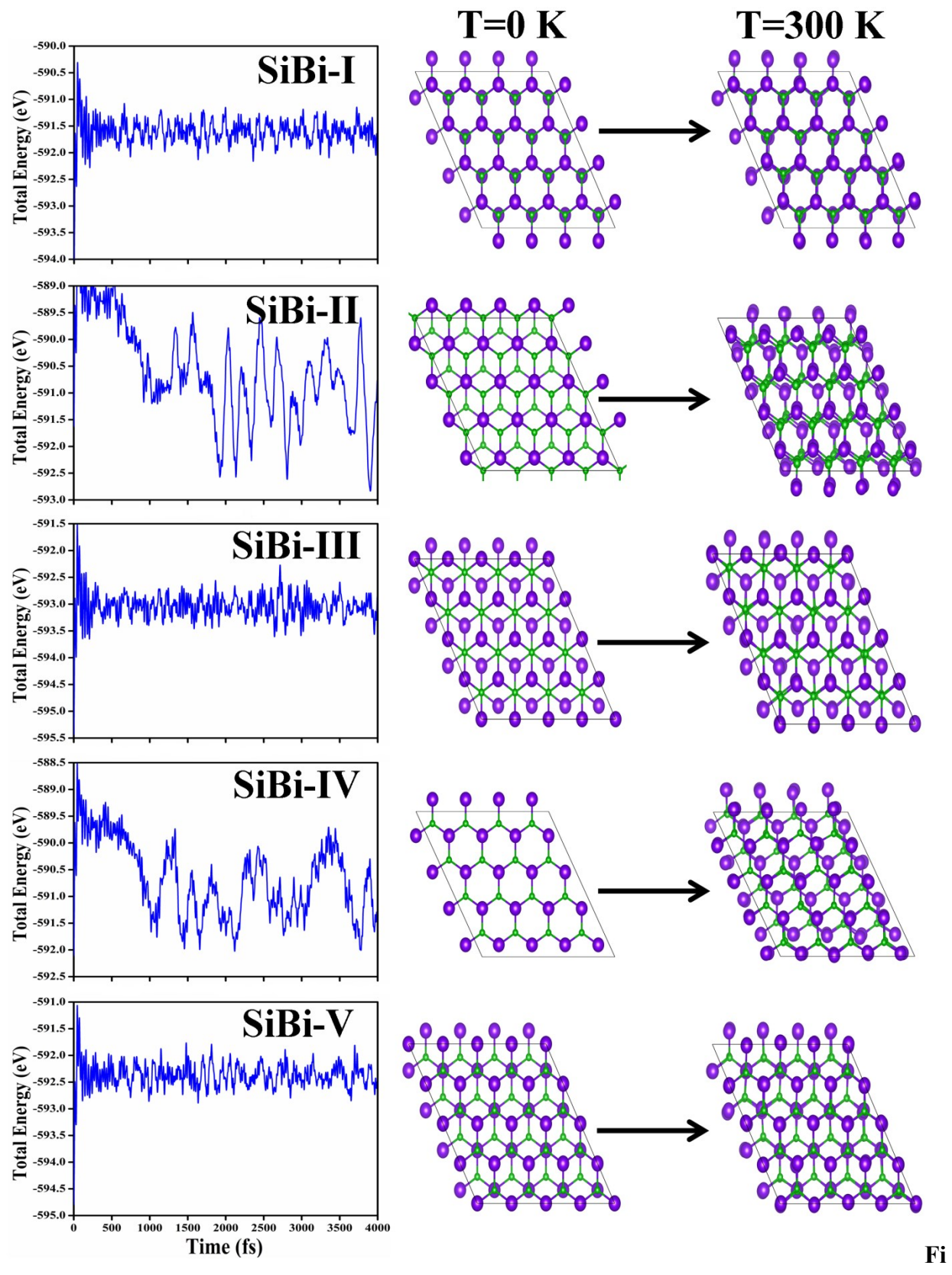
g. S3(b)



ig. S3(c)



ig. S3(d)



g. S3(e)

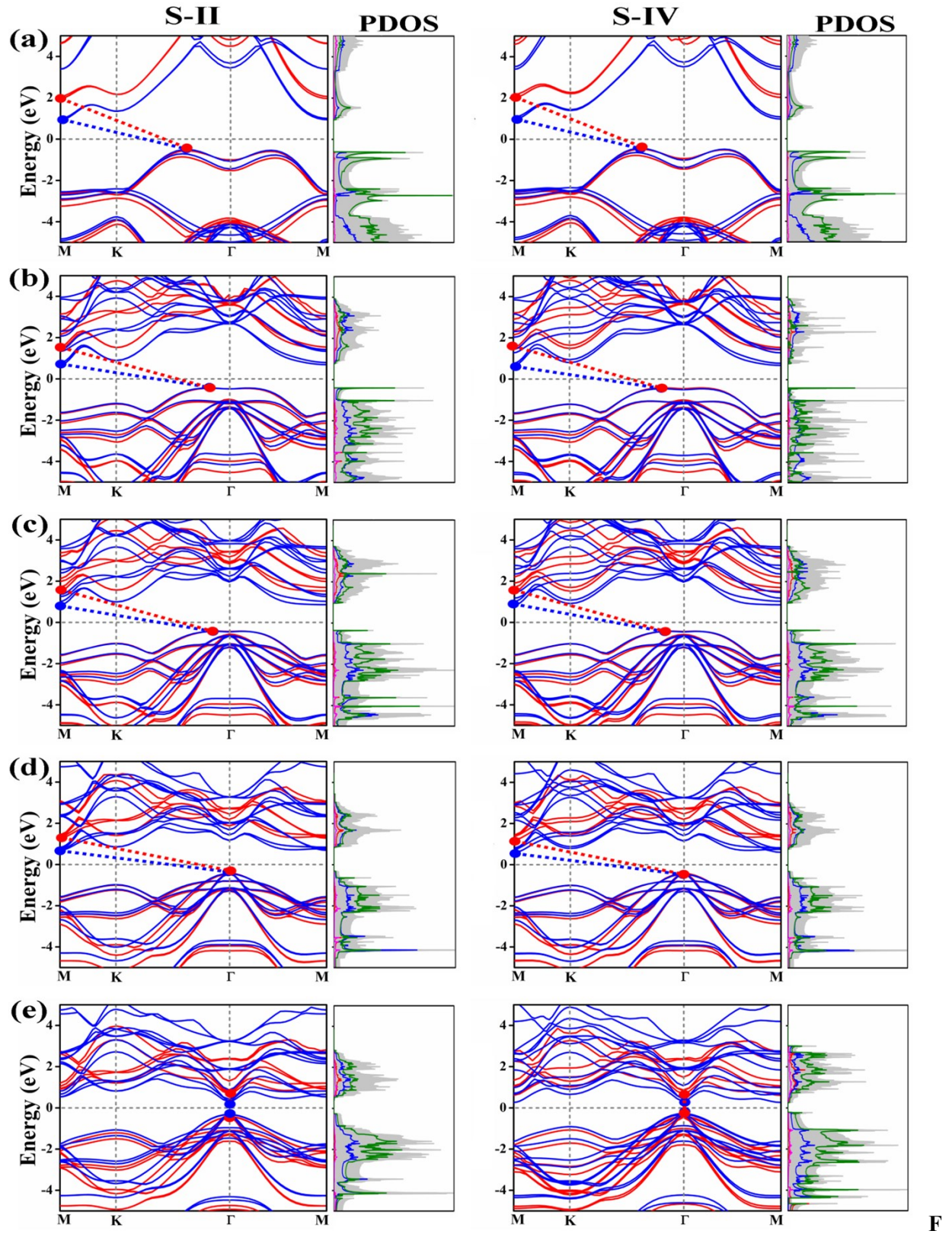


fig. S4

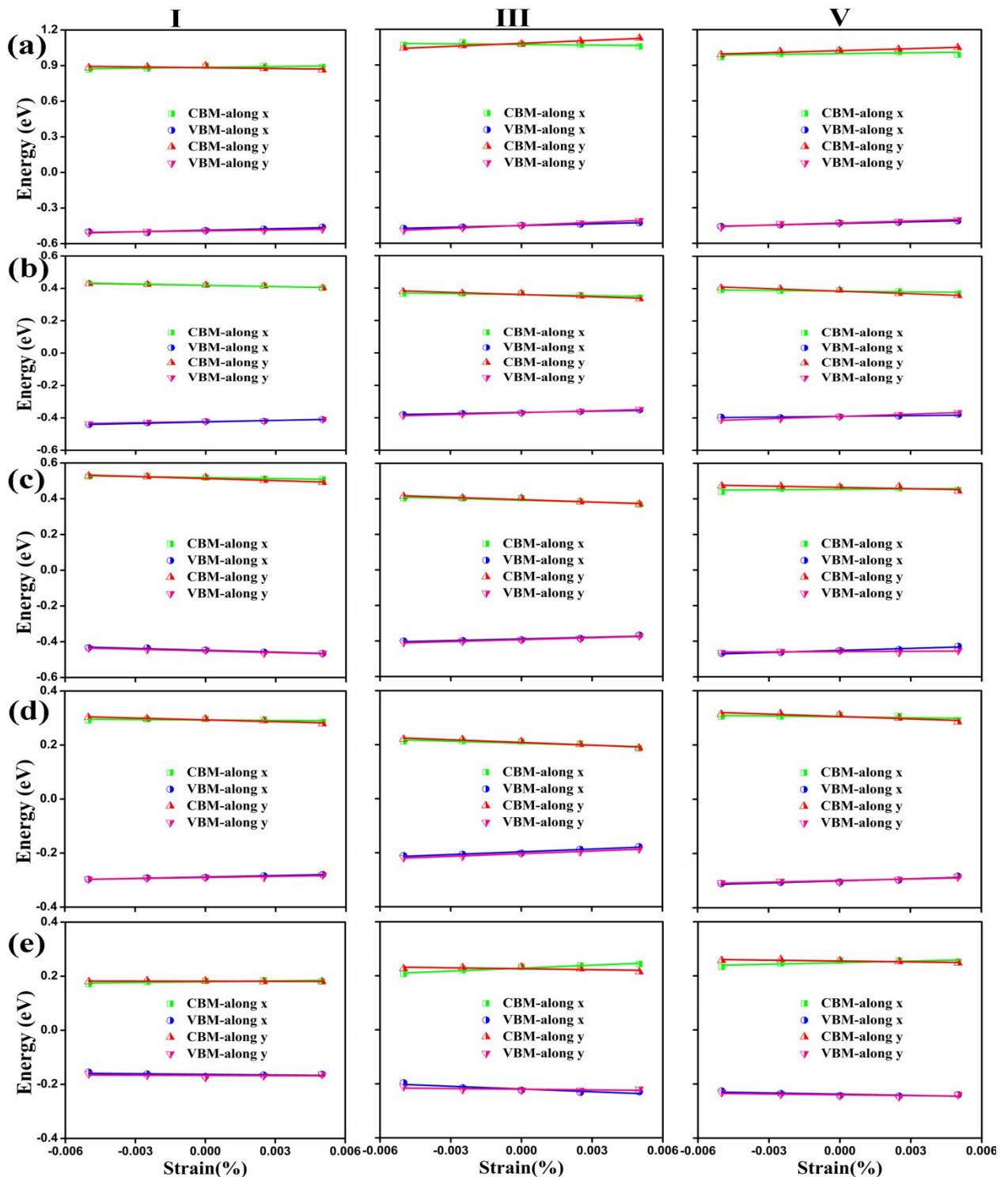


Fig. S5

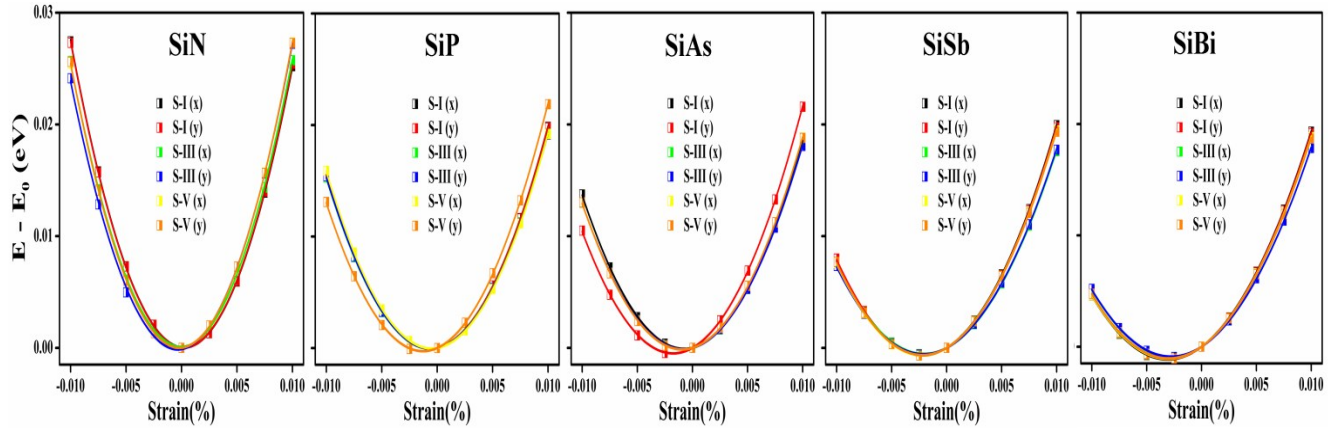


Fig. S6

OER/ORR Mechanism:

The adsorption energies consisting of oxygen intermediates for the oxygen evolution reaction (OER) and oxygen reduction reaction (ORR) are calculated using;

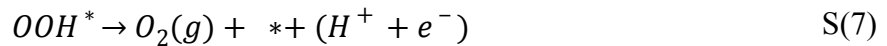
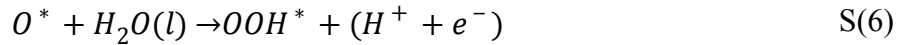
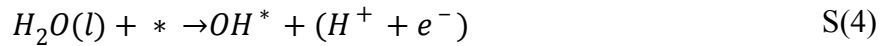
$$\Delta E_{O^*} = E_{O^*} - E_{\text{active site}} - (E_{H_2O} - E_{H_2}) \quad \text{S(1)}$$

$$\Delta E_{OH^*} = E_{OH^*} - E_{\text{active site}} - (E_{H_2O} - \frac{1}{2}E_{H_2}) \quad \text{S(2)}$$

$$\Delta E_{OOH^*} = E_{OOH^*} - E_{\text{active site}} - (2E_{H_2O} - \frac{3}{2}E_{H_2}) \quad \text{S(3)}$$

Here, * represents the active site. The total energies in free gas phase of H₂O and H₂ molecules are represented as E_{H_2O} and E_{H_2} respectively. The total energies of the active site (*) with the adsorption of O, OH, and OOH are represented as E_{O^*} , E_{OH^*} , and E_{OOH^*} respectively.

Under acidic conditions, the OER and ORR process with four-electron reaction paths is expressed as-



Here, the gas and liquid phases are indicated by g and l respectively; * indicates the absorption site on the catalyst surface and the absorbed intermediates are represented by O^* , OH^* and OOH^* . The opposite process of OER is the ORR reaction as listed from Equ. S(4)-S(7).

Table. S6

| Homo-bilayers | position | E_{ad} (eV) | | |
|----------------------|-----------------|----------------------------|------------|-------------|
| | | O* | OH* | OOH* |
| SiP | On-Si | 2.24 | 1.13 | 1.70 |
| | On-P | 0.79 | 0.93 | 3.10 |
| SiAs | On-Si | 2.64 | 1.12 | 5.11 |
| | On-As | 2.01 | 1.53 | 4.97 |

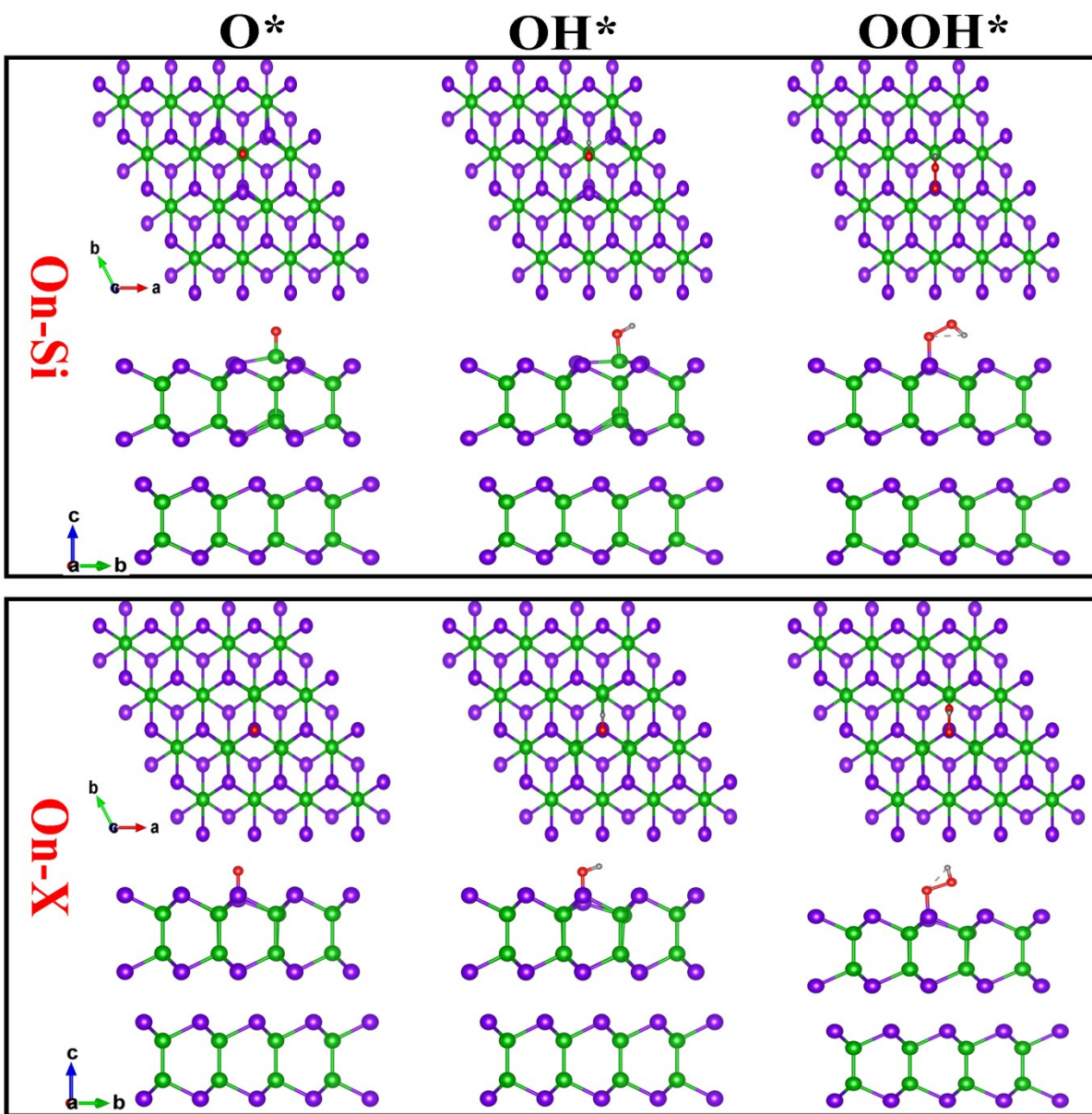


Fig. S7

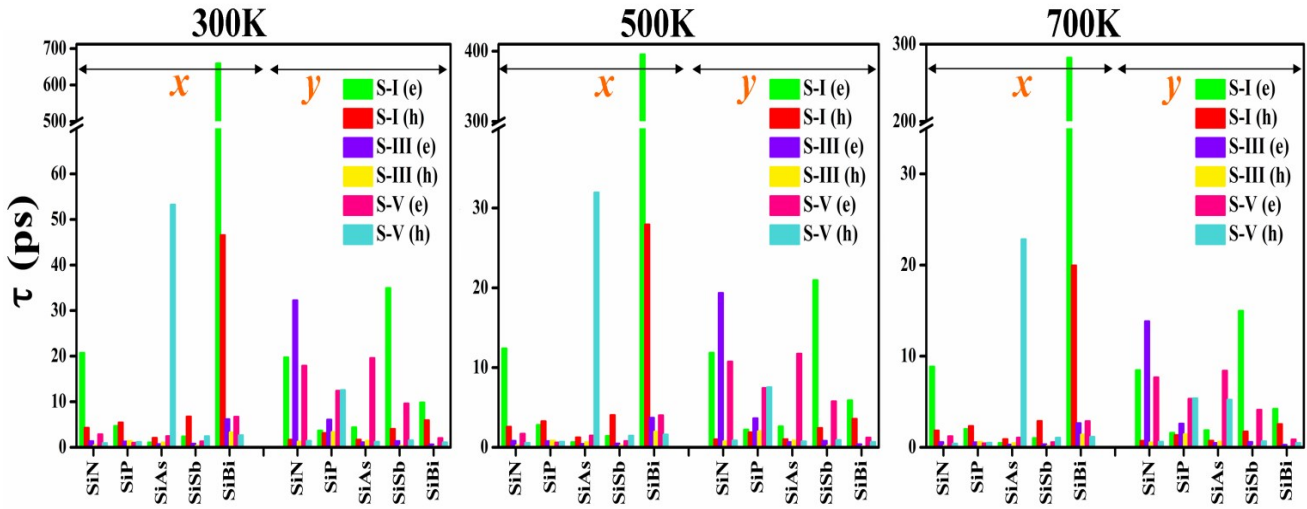


Fig. S8

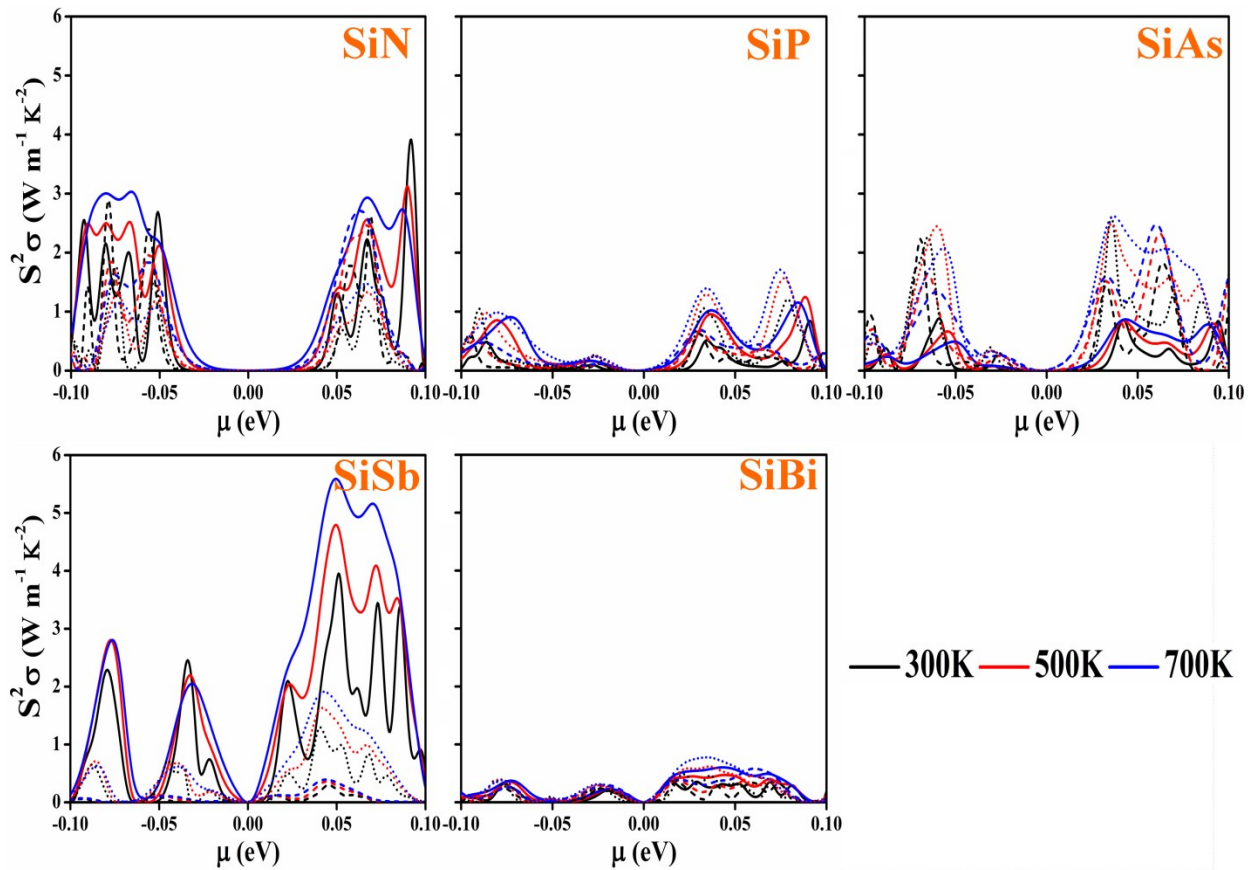


Fig. S9